

Cavity quantum electrodynamics with a single quantum dot coupled to a photonic molecule

Arka Majumdar,^{*} Armand Rundquist, Michal Bajcsy, and Jelena Vučković*E. L. Ginzton Laboratory, Stanford University, Stanford, California 94305, USA*

(Received 30 January 2012; published 18 July 2012)

We demonstrate the effects of cavity quantum electrodynamics for a quantum dot coupled to a photonic molecule consisting of a pair of coupled photonic crystal cavities. We show anticrossing between the quantum dot and the two supermodes of the photonic molecule, signifying achievement of the strong coupling regime. From the anticrossing data, we estimate the contributions of both mode-coupling and intrinsic detuning to the total detuning between the supermodes. Finally, we also show signatures of off-resonant cavity-cavity interaction in the photonic molecule.

DOI: [10.1103/PhysRevB.86.045315](https://doi.org/10.1103/PhysRevB.86.045315)

PACS number(s): 42.50.Pq, 42.70.Qs

I. INTRODUCTION

A single quantum emitter coupled to a resonator constitutes a cavity quantum electrodynamic (cQED) system for studying strong light-matter interaction. With an eye toward achieving a scalable quantum computer¹ and more recently a photonic quantum simulator²⁻⁴ significant progress has been achieved in optical cQED as well as its microwave counterpart circuit QED. One such cQED system consisting of a single quantum dot (QD) coupled to a photonic crystal (PC) cavity has recently emerged as an attractive candidate for integrated nanophotonic quantum information processing devices.⁵ This solid-state cQED system is of considerable interest to the quantum optics community for the generation of nonclassical states of light,^{6,7} for its application to all-optical^{8,9} and electro-optical switching,¹⁰ and due to unusual effects like the off-resonant dot-cavity interaction due to electron-phonon coupling.¹¹ However, all of the cQED effects demonstrated so far in this system involve a single cavity. Although numerous theoretical proposals employing multiple cavities coupled to single quantum emitters exist in the cQED and circuit-QED literature,^{2-4,12} experimental development in this direction is rather limited. Most of these proposals, for example, observing the quantum phase transition of light, require a nonlinearity in each cavity, which is a formidable task with current technology. However, several proposals involving a single QD coupled to multiple cavities predict novel quantum phenomena, for example, generation of bound photon-atom states¹³ or sub-Poissonian light generation in a pair of coupled cavities or in a photonic molecule containing a single QD.^{14,15} This photonic molecule, coupled to a single QD, forms the first step toward building an integrated cavity network with coupled QDs. Photonic molecules made of PC cavities were studied previously^{16,17} to observe mode-splitting due to coupling between the cavities. In those studies, a high density of QDs was used merely as an internal light source to generate photoluminescence (PL) under above-band excitation and no quantum properties of the system were studied. In another experiment, a photonic molecule consisting of two micropost cavities was used along with a single QD to generate entangled photons via exciton-biexciton decay, but the QD-cavity system was in the weak coupling regime and the Purcell enhancement was the only cQED effect observed.¹⁸ In addition to the photonic molecule, fabrication of large-scale coupled cavities (without any quantum emitters) have been reported both in

photonic crystal platform¹⁹ and in circuit QED,²⁰ revealing the widespread interest in exploring the scalability of these systems.

In this paper, we demonstrate strong coupling of a photonic molecule with a single QD. We note that even though the photonic molecule described in this paper is based on photonic crystal optical microcavities, one can also employ Fabry Perot cavities, DBR microcavities, microposts or microwave cavities^{20,21} for this task. However, to best of our knowledge, coupling multiple cavities to single quantum emitters has not been shown in any other cQED system. We show clear anticrossing between the QD and two supermodes formed in the photonic molecule. In general, the exact coupling strength between two cavities in a photonic molecule is difficult to calculate, as the observed separation between the two modes has contributions both from the cavity coupling strength as well as from the mismatch between the two cavities due to fabrication imperfections. However, by monitoring the interaction between a single QD and the photonic molecule we can exactly calculate the coupling strength between the cavities and separate the contribution of the bare detuning due to cavity mismatch. In fact, without any coupling between two cavities, one cannot have strong coupling of the QD with both of the observed modes. Hence, the observed anticrossing of the QD with both modes clearly indicates coupling between the cavities. Apart from the strong coupling, we also demonstrate off-resonant phonon-mediated interaction between the two cavity modes, a recently found effect in solid-state cavity systems.²²

II. THEORY

Let us consider a photonic molecule consisting of two cavities with annihilation operators for their bare (uncoupled) modes denoted by a and b , respectively. We assume that a QD is placed in and resonantly coupled to the cavity described by operator a . The Hamiltonian describing such a system is

$$\mathcal{H} = \Delta_o b^\dagger b + J(a^\dagger b + ab^\dagger) + g(a^\dagger \sigma + a \sigma^\dagger), \quad (1)$$

where Δ_o is the detuning between the two bare cavity modes; J and g are, respectively, the intercavity and dot-cavity coupling strength; σ is the QD lowering operator; and the resonance frequency ω_0 of the cavity with annihilation operator a is assumed to be zero. We now transform this Hamiltonian by mapping the cavity modes a and b to the bosonic modes α and

β introduced as $a = \cos(\theta)\alpha + \sin(\theta)\beta$ and $b = \sin(\theta)\alpha - \cos(\theta)\beta$. We note that this mapping maintains the appropriate commutation relations between operators a and b . Under these transformations we can decouple the two cavity modes (α and β) for the following choice of θ :

$$\tan(2\theta) = -\frac{2J}{\Delta_o}. \quad (2)$$

Under this condition the transformed Hamiltonian becomes

$$\mathcal{H} = \alpha^\dagger \alpha [\Delta_o \sin^2(\theta) + J \sin(2\theta)] + g \cos(\theta) (\alpha^\dagger \sigma + \alpha \sigma^\dagger) + \beta^\dagger \beta [\Delta_o \cos^2(\theta) - J \sin(2\theta)] + g \sin(\theta) (\beta^\dagger \sigma + \beta \sigma^\dagger).$$

Therefore, a QD coupled to a photonic molecule has exactly the same eigenstructure as two detuned cavities with the QD coupled to both of them (from the equivalence of the two expressions above for the Hamiltonian \mathcal{H}). The supermodes of the transformed Hamiltonian α and β will be separated by $\Delta = \sqrt{\Delta_o^2 + 4J^2}$ [obtained by subtracting the terms multiplying $\alpha^\dagger \alpha$ and $\beta^\dagger \beta$, under the conditions of Eq. (2)] and the interaction strength between the QD and the supermodes will be $g_1 = g \cos(\theta)$ and $g_2 = g \sin(\theta)$. Hence, $g = \sqrt{g_1^2 + g_2^2}$, $\theta = \arctan(g_2/g_1)$, and so $\tan(2\theta) = 2g_1 g_2 / (g_1^2 - g_2^2) = -2J/\Delta_o$. If the two cavities are not coupled ($J = 0$ and $\theta = 0$), we can still observe two different cavity modes in the experiment due to Δ_o , the intrinsic detuning between two bare cavities. However, if we tune the QD across the two cavities in this case, we will observe QD-cavity interaction only with one cavity mode [in this case α , as the term coupling β to the QD in the transformed Hamiltonian will vanish, as a result of $\sin(\theta) = 0$]. In other words, in this case the QD is spatially located in only one cavity and cannot interact with the other, spatially distant and decoupled cavity. Figure 1 shows the numerically calculated cavity transmission spectra (proportional to $\langle a^\dagger a \rangle + \langle b^\dagger b \rangle$) when the QD is tuned across the two cavity resonances. When the two cavities are coupled ($J \neq 0$), we observe anticrossing between each cavity mode and the QD [Fig. 1(a)]. However, only one anticrossing is observed when the cavities are not coupled [Fig. 1(b)].

III. CHARACTERIZATION OF PHOTONIC MOLECULE

The actual experiments are performed with self-assembled InAs QDs embedded in GaAs, and the whole system is kept at cryogenic temperatures (~ 10 – 25 K) in a helium-flow cryostat. The cavities used are linear three-hole defect GaAs PC cavities coupled via spatial proximity. The photonic crystal is fabricated from a 160-nm-thick GaAs membrane, grown by molecular beam epitaxy on top of a GaAs (100) wafer. A low-density layer of InAs QDs is grown in the center of the membrane (80 nm beneath the surface). The GaAs membrane sits on a 918-nm sacrificial layer of $\text{Al}_{0.8}\text{Ga}_{0.2}\text{As}$. Under the sacrificial layer, a 10-period distributed Bragg reflector, consisting of a quarter-wave AlAs/GaAs stack, is used to increase collection into the objective lens. The photonic crystal was fabricated using electron beam lithography, dry plasma etching, and wet etching of the sacrificial layer in diluted hydrofluoric acid, as described previously.^{11,23}

We fabricated two different types of coupled cavities: in one case, the two cavities are offset at a 60° angle [inset of Fig. 2(a)] and in the other the two cavities are laterally coupled

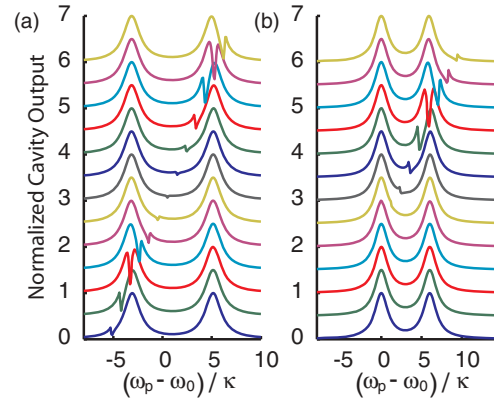


FIG. 1. (Color online) Numerically calculated cavity transmission spectra when the QD resonance is tuned across the two cavity resonances. (a) Anticrossing is observed between the quantum dot and both cavity modes when the two cavities are coupled (coupling rate between the two cavities is $J/2\pi = 80$ GHz). (b) When the two cavities are not coupled ($J = 0$), we observe anticrossing in only one cavity. Parameters used for the simulation: cavity decay rate $\kappa/2\pi = 20$ GHz (for both cavities); QD dipole decay rate $\gamma/2\pi = 1$ GHz; dot-cavity coupling rate of $g/2\pi = 10$ GHz; intrinsic detuning between the bare cavity modes $\Delta_o/2\pi = 40$ GHz for (a) and 120 GHz for (b). The plots are vertically offset for clarity. The horizontal axis corresponds to the detuning of the probe laser frequency ω_p from the cavity a resonance ω_0 in units of cavity field decay rate.

[inset of Fig. 2(b)]. In the first case the coupling between the cavities is stronger as the overlap between the electromagnetic fields confined in the cavities is larger along the 60° angle. Figures 2(a) and 2(b) show the typical PL spectra of these two different types of coupled cavities for different spacing

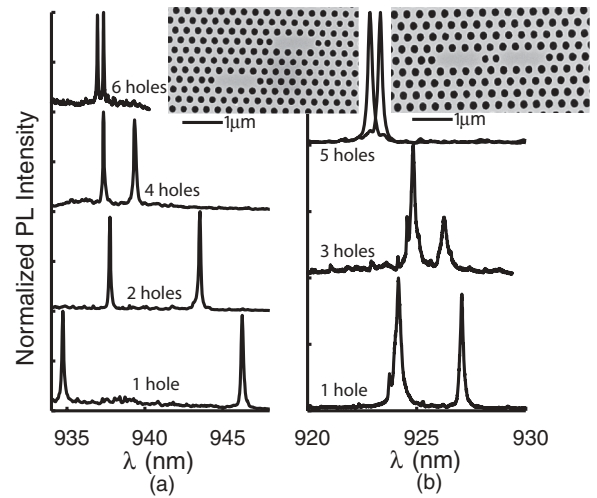


FIG. 2. Photoluminescence spectra of the coupled cavities for different hole spacings between two cavities: (a) the cavities are separated at an angle of 60° [see the inset for a scanning electron micrograph (SEM)]; (b) the cavities are laterally separated (see the inset for SEM). A decrease in the wavelength separation between two cavity modes is observed with increasing spatial separation between the cavities (i.e., with increasing number of holes inserted in between the two cavities). A much larger separation is observed in (a) when the cavities are coupled at an angle compared to the lateral coupling (b).

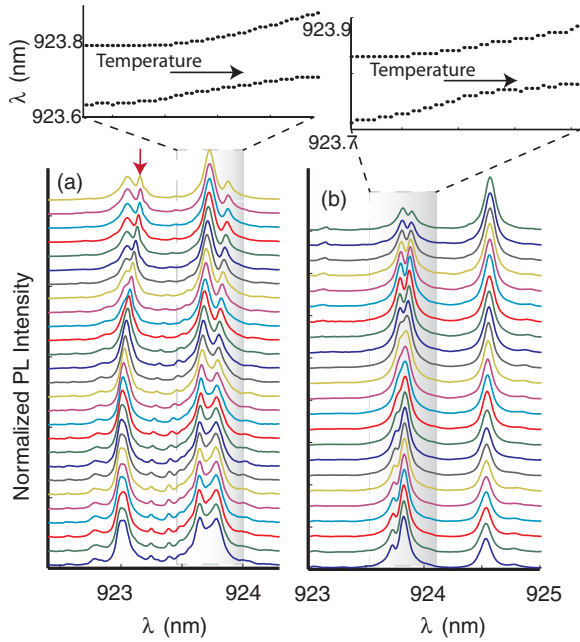


FIG. 3. (Color online) Normalized PL intensity plotted when we tune the QD across the cavity resonance by temperature: (a) before nitrogen deposition (i.e., the QD is temperature tuned across the longer wavelength resonance) and (b) after nitrogen deposition (which red-shifts the cavity resonances and allows us to temperature tune the QD across the shorter wavelength resonance). Clear anticrossings between the QD and the cavity are observed for both supermodes. In both cases, the temperature is increased from bottom to top (the plots are vertically offset for clarity). In the inset the resonances of the two anticrossing peaks (as extracted from curve fitting) are plotted. Clear anticrossing is observed in both cases.

between the cavities. A clear decrease in the frequency separation between the cavities is observed with increasing spatial separation. Note that the consistency of this trend between different fabrication runs already indicates that this frequency separation cannot be purely due to the fabrication-related intrinsic detuning between the two cavities. Nevertheless, it is very difficult to quantify how much of the separation is due to coupling (J) and how much is due to intrinsic detuning (Δ_o) of the cavity resonances. However, we will show that by observing the anticrossing between the QD and the two modes we can conclusively determine both J and Δ_o .

IV. STRONG COUPLING WITH A SINGLE QD

First, we investigate the strong coupling between a single QD and the photonic molecule in PL. For this particular experiment, we used a photonic molecule consisting of cavities separated by four holes along the 60° angle. In practice it is not trivial to tune the QD over such a long wavelength range as required by the observed separation of the two cavity peaks. Hence, we use two different tuning techniques: We tune the cavity modes by depositing nitrogen on the cavity,²⁴ and then tune the QD resonance across the cavity resonance by changing the temperature of the system. For Fig. 3(a) there is no nitrogen deposition and the temperature is changed from 20 K to 30 K to tune the QD across the longer-wavelength cavity mode. For Fig. 3(b) we deposited

nitrogen (to red-shift cavities) and changed the temperature from 20 K to 40 K, showing the anticrossing between the QD and the shorter-wavelength cavity mode. We note that all these temperatures are measured at the cold-finger of the cryostat. We observe less shift of the cavity resonance with temperature after nitrogen deposition, most likely because the nitrogen starts evaporating with increasing temperature causing the cavity to blue-shift, thus compensating for the red-shift caused by increased temperature. We fit the PL spectra to find the resonances of coupled QD-cavity system and plot the resonances in the inset of Figs. 3(a) and 3(b). We observe clear anticrossings for both coupled modes. The nitrogen and the temperature tuning do not cause a significant change in the coupling and the detuning between the cavities, as confirmed in the experiments described below. We note that there is another QD (shown by the red arrow) in Fig. 3(a) weakly coupled to the cavity as no anticrossing between that QD and the cavity is observed. Within the cavity region, we typically have about four QDs that are spectrally distributed over a wide range. Spatially, they are also distributed within the cavity and, thus, have different coupling strengths to the cavity mode. Tuning the system over a large range of wavelengths (as we do in this experiment, with temperature and nitrogen tuning) can bring into resonance some of these other QDs, as shown by this additional peak. However, no signature of coupling between this QD and the QD under study for anticrossing is observed, and the presence of this additional weakly coupled dot does not change the conclusions of the experiment. Finally, the additional QD is not visible in Fig. 3(b), as it is off-resonant from both cavity modes.

We perform curve fitting for the PL spectra when the QD is resonant to the cavity super-modes and estimate the system parameters [Figs. 4(a) and 4(b)]. The supermode at shorter (longer) wavelength is denoted as sm1 (sm2). As the detuning between the supermodes is much larger than the vacuum Rabi splitting caused by the QD, we can assume that when the QD is resonant to sm1(2), its interaction with sm2(1) is negligible. Therefore, we can fit the PL spectra of sm1

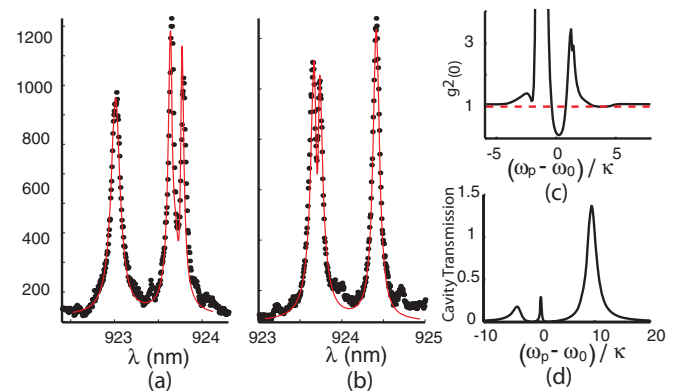


FIG. 4. (Color online) QD-photonic molecule spectrum, (a) when the QD is resonant with super-mode sm2 and (b) when the QD is resonant with supermode sm1. From the fit we extract the system parameters (see text). Numerically simulated (c) second-order autocorrelation $g^2(0)$ and (d) transmission from cavity b , as a function of laser frequency, with the experimental system parameters that were extracted from the fits.

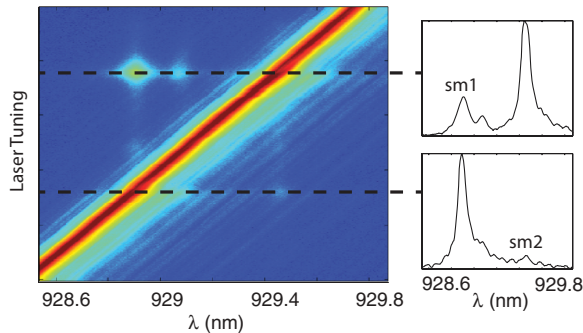


FIG. 5. (Color online) Off-resonant interaction between two coupled cavities and a QD. We scan the laser across both coupled modes and observe emission from the off-resonant supermode, under excitation of the other supermode. A close-up spectrum for each resonance shows the relative position of the laser and the cavity modes.

(sm2) modes exhibiting Rabi splitting individually. For sm1, we extract from the fit the field decay rate $\kappa_1/2\pi = 22.4$ GHz and the QD-field interaction strength $g_1/2\pi = 14.2$ GHz [Fig. 4(b)]; for sm2, $\kappa_2/2\pi = 16.7$ GHz and $g_2/2\pi = 23.7$ GHz [Fig. 4(a)]. We note that we can achieve very high quality factors (~ 7000 – 10000) of the coupled cavity modes as seen from the extracted κ values. We also estimate the total detuning between two observed modes as $\Delta/2\pi \sim 246.5$ and 253.5 GHz before and after nitrogen tuning. This minimal difference in Δ resulting from the nitrogen tuning does not impact our further analysis, and we take Δ to be the average of these two values. The change in the cavity field decay rates arising from the nitrogen deposition is also minimal. From these data, we use the relations $2g_1g_2/(g_1^2 - g_2^2) = -2J/\Delta_o$ and $\Delta = \sqrt{4J^2 + \Delta_o^2}$ (previously derived in the paper) to obtain $J/2\pi \approx 110$ GHz and $\Delta_o/2\pi \approx 118$ GHz.

We now numerically simulate the performance of such a QD-photonic molecule for generation of sub-Poissonian light using the quantum optical master equation approach.²⁵ Two bare cavity modes are separated by $\Delta_o/2\pi = 118$ GHz; a QD is resonant and strongly coupled to one of the modes (*a*) with interaction strength $g/2\pi = 27.6$ GHz (as discussed earlier, $g = \sqrt{g_1^2 + g_2^2}$, where g_1 and g_2 are the two values of QD-cavity interaction strengths obtained by fitting the PL spectra); mode *b* is the empty cavity. The mode *b* is driven and the second order autocorrelation $g^2(0) = \frac{\langle b^{\dagger}b^{\dagger}bb \rangle}{\langle b^{\dagger}b \rangle^2}$ of the transmitted light through cavity *b* is calculated.¹⁵ We also assume the two cavities to have the same cavity decay rate, which is an average of the cavity decay rates measured from the two supermodes. Note, however, that having slightly different decay rates does not significantly affect the performance of the system. The numerically simulated cavity *b* transmission and $g^2(0)$ of the transmitted light is shown in Figs. 4(c) and 4(d). From these simulated data, we observe that with our system

parameters we should be able to achieve strongly sub-Poissonian light with $g^2(0) \sim 0.03$. Unfortunately, in practice it is very difficult to drive only one cavity mode without affecting the other mode due to the spatial proximity of two cavities. This individual addressability is critical for good performance of the system¹⁵ and to retain such a capability in a photonic molecule the cavities should be coupled via a waveguide.²⁶

V. OFF-RESONANT COUPLING

Finally, as a further demonstration of cQED effects in this system, we report off-resonant interaction between the coupled cavities and the QD, similar to the observations in a single linear three-hole defect cavity²² and a nano-beam cavity.²⁷ This experiment was performed on a different QD-photonic molecule system than the one where we observed strong coupling. Figure 5 shows the spectra indicating off-resonant coupling between the cavities and the QD. Under resonant excitation of the supermode at longer wavelength (sm2), we see pronounced emission from both sm1 and a nearby QD. Similarly, under resonant excitation of sm1, we see emission from sm2, although the emission is much weaker. We exclude the presence of any nonlinear optical processes by performing a laser-power-dependent study of the cavity emission, which shows a linear dependence of the cavity emission on the laser power (not shown here).

VI. CONCLUSION

In summary, we demonstrated strong coupling of a single QD to a photonic molecule in a photonic crystal platform. Clear anticrossings between the QD and both supermodes of the photonic molecule were observed, showing conclusive evidence of intercavity coupling. From the anticrossing data we were able to separate the contributions of the intercavity coupling and intrinsic detuning to the cavity mode splitting. We have also reported observation of off-resonant cavity-cavity and cavity-QD interaction in this type of system. Such a system could be employed for nonclassical light generation (as theoretically studied in this article) and represents a building block for an integrated nanophotonic network in a solid-state cQED platform.

ACKNOWLEDGMENTS

The authors acknowledge financial support provided by the Office of Naval Research (PECASE Award; No: N00014-08-1-0561), DARPA (Award No: N66001-12-1-4011), NSF (DMR-0757112), and Army Research Office (W911NF-08-1-0399). A.R. is also supported by a Stanford Graduate Fellowship. We acknowledge Dr. Hyochul Kim and Dr. Pierre Petroff for providing the quantum dot sample. This work was performed in part at the Stanford Nanofabrication Facility of NNIN, supported by the National Science Foundation.

*arkam@stanford.edu

¹L.-M. Duan and H. J. Kimble, *Phys. Rev. Lett.* **92**, 127902 (2004).

²M. J. Hartmann, F. G. S. L. Brandao, and M. B. Plenio, *Nat. Phys.* **2**, 849 (2006).

³A. D. Greentree, C. Tahan, J. H. Cole, and L. C. L. Hollenberg, *Nat. Phys.* **2**, 856 (2006).

⁴A. A. Houck, H. E. Treci, and J. Koch, *Nat. Phys.* **8**, 292 (2012).

- ⁵A. Faraon, A. Majumdar, D. Englund, E. Kim, M. Bajcsy, and J. Vučković, *New J. Phys.* **13**, 055025 (2011).
- ⁶A. Faraon, I. Fushman, D. Englund, N. Stoltz, P. Petroff, and J. Vučković, *Nat. Phys.* **4**, 859 (2008).
- ⁷A. Majumdar, M. Bajcsy, and J. Vučković, *Phys. Rev. A* **85**, 041801(R) (2012).
- ⁸D. Englund, A. Majumdar, M. Bajcsy, A. Faraon, P. Petroff, and J. Vučković, *Phys. Rev. Lett.* **108**, 093604 (2012).
- ⁹R. Bose, D. Sridharan, H. Kim, G. S. Solomon, and E. Waks, *Phys. Rev. Lett.* **108**, 227402 (2012).
- ¹⁰A. Faraon, A. Majumdar, H. Kim, P. Petroff, and J. Vučković, *Phys. Rev. Lett.* **104**, 047402 (2010).
- ¹¹D. Englund, A. Majumdar, A. Faraon, M. Toishi, N. Stoltz, P. Petroff, and J. Vučković, *Phys. Rev. Lett.* **104**, 073904 (2010).
- ¹²I. Carusotto, D. Gerace, H. E. Tureci, S. De Liberato, C. Ciuti, and A. Imamoglu, *Phys. Rev. Lett.* **103**, 033601 (2009).
- ¹³P. Longo, P. Schmitteckert, and K. Busch, *Phys. Rev. Lett.* **104**, 023602 (2010).
- ¹⁴T. C. H. Liew and V. Savona, *Phys. Rev. Lett.* **104**, 183601 (2010).
- ¹⁵M. Bamba, A. Imamoglu, I. Carusotto, and C. Ciuti, *Phys. Rev. A* **83**, 021802 (2011).
- ¹⁶K. A. Atlasov, K. F. Karlsson, A. Rudra, B. Dwir, and E. Kapon, *Opt. Express* **16**, 16255 (2008).
- ¹⁷K. A. Atlasov, A. Rudra, B. Dwir, and E. Kapon, *Opt. Express* **19**, 2619 (2011).
- ¹⁸A. Dousse, J. Suffczynski, A. Beveratos, O. Krebs, A. Lematre, I. Sagnes, J. Bloch, P. Voisin, and P. Senellart, *Nature* **466**, 217 (2010).
- ¹⁹M. Notomi, E. Kuramochi, and T. Tanabe, *Nat. Photon.* **2**, 741 (2008).
- ²⁰D. Underwood, W. S. Jens Koch, and A. A. Houck, *arXiv:1203.5363* (2012).
- ²¹C. D. Ogden, E. K. Irish, and M. S. Kim, *Phys. Rev. A* **78**, 063805 (2008).
- ²²A. Majumdar, A. Faraon, E. D. Kim, D. Englund, H. Kim, P. Petroff, and J. Vučković, *Phys. Rev. B* **82**, 045306 (2010).
- ²³D. Englund, A. Faraon, I. Fushman, N. Stoltz, P. Petroff, and J. Vučković, *Nature* **450**, 857 (2007).
- ²⁴S. Mosor, J. Hendrickson, B. C. Richards, J. Sweet, G. Khitrova, H. M. Gibbs, T. Yoshie, A. Scherer, O. B. Shchekin, and D. G. Deppe, *Appl. Phys. Lett.* **87**, 141105 (2005).
- ²⁵A. Majumdar, E. D. Kim, Y. Gong, M. Bajcsy, and J. Vučković, *Phys. Rev. B* **84**, 085309 (2011).
- ²⁶Y. Sato, Y. Tanaka, J. Upham, Y. Takahashi, T. Asano, and S. Noda, *Nat. Photon.* **6**, 5661 (2012).
- ²⁷A. Rundquist, A. Majumdar, and J. Vučković, *Appl. Phys. Lett.* **99**, 251907 (2011).